

## RESEARCH ARTICLE

# The impact of UVB radiation on the glycoprotein glue of orb-weaving spider capture thread

Sarah D. Stellwagen\*, Brent D. Opell and Mary E. Clouse

## ABSTRACT

Many spider orb-webs are exposed to sunlight and the potentially damaging effects of ultraviolet B (UVB) radiation. We examined the effect of UVB on the viscoelastic glycoprotein core of glue droplets deposited on the prey capture threads of these webs, hypothesizing that webs built by species that occupy sunny habitats are less susceptible to UVB damage than are webs built by species that prefer shaded forest habitats or by nocturnal species. Threads were tested shortly after being collected in the early morning and after being exposed to UVB energy equivalent to a day of summer sun and three times this amount. Droplets kept in a dark chamber allowed us to evaluate post-production changes. Droplet volume was unaffected by treatments, indicating that UVB did not damage the hygroscopic compounds in the aqueous layer that covers droplets. UVB exposure did not affect energies of droplet extension for species from exposed and partially to mostly shaded habitats (*Argiope aurantia*, *Leucauge venusta* and *Verrucosa arenata*). However, UVB exposure reduced the energy of droplet extension in *Micrathena gracilis* from shaded forests and *Neoscona crucifera*, which forages at night. Only in *L. venusta* did the energy of droplet extension increase after the dark treatment, suggesting endogenous molecular alignment. This study adds UVB irradiation to the list of factors (humidity, temperature and strain rate) known to affect the performance of spider glycoprotein glue, factors that must be more fully understood if adhesives that mimic spider glycoprotein glue are to be produced.

**KEY WORDS:** Adhesion, Biomaterials, Toughness, Silk, Ultraviolet

## INTRODUCTION

Ultraviolet radiation (UVR) introduces free radical oxidative stress to organisms and biological materials, resulting in damaged cellular components including DNA and proteins (Tyrrell, 1995; Osaki and Osaki, 2011; Kaur et al., 2013; Matsuhira et al., 2013). Marine and terrestrial organisms have adapted to prevent and cope with such UVR exposure and damage. These adaptations can be behavioral, such as moving into the shade (Gleason et al., 2006; Ma et al., 2013), physiological, such as absorptive pigmentation like melanin (Singaravelan et al., 2008) and mycosporine-like amino acids (MAAs) (Kuffner, 2002; Hylander and Hansson, 2013), or biochemical such as molecular repair (Carlson and Smith, 1981; Connelly et al., 2009) and antioxidants (Swindells and Rhodes, 2004; Hudelson, 2011).

Some organisms, like the orb-weaving spider *Argiope aurantia* Lucas 1833, remain exposed to full sunlight during the day throughout the late summer and early autumn (Harwood, 1974).

These spiders produce aerial silk webs to catch and retain flying insects. Their webs consist of radial threads that support a spiral of capture silk, which incorporates adhesive glue droplets (Apstein, 1889; Sekiguchi, 1952; Sahni et al., 2014). Each transparent droplet is composed of an inner sticky, viscoelastic glycoprotein core (Sahni et al., 2010), covered by an aqueous, hygroscopic outer covering that maintains moisture levels (Fig. 1; Edmonds and Vollrath, 1992). Most species spin webs in the early morning hours, monitor them using a sit-and-wait strategy throughout the day, and recycle their silk when a new web is produced the next day (Reed et al., 1969).

Viscous capture thread originates from a pair of posterior lateral spinnerets on a spider's abdomen. A triad of spigots on each spinneret includes a central spigot that produces the flagelliform supporting axial strand while a pair of surrounding aggregate spigots secretes the glue. The coated strands from each spinneret then join to form a proto-viscous thread. The glue first forms a continuous cylinder around the axial fibers, but after rapidly absorbing atmospheric moisture, swells to create surface tension that quickly separates the material into droplets (Fig. 1A; Plateau, 1873; Boys, 1889; Strutt, 1892; Edmonds and Vollrath, 1992). Each droplet is composed of a glycoprotein core (Opell and Hendricks, 2010), which confers stickiness (Sahni et al., 2010), surrounded by a hygroscopic aqueous layer that also extends into inter-droplet regions (Fig. 1). At the center of the glycoprotein core, a denser region termed a granule can often be seen in transmitted light images of flattened droplets (Opell and Hendricks, 2010). This granule is hypothesized to be a region where the glycoprotein is anchored to the axial lines, causing it to resist forces that would slide a droplet along these lines. The epi-illumination used in subsequent studies to more clearly reveal the outline of a droplet's glycoprotein core (e.g. Opell et al., 2013; Stellwagen et al., 2014) makes it difficult to visualize these granules independently of the surrounding glycoprotein core within flattened droplets (Fig. 1C).

Inorganic and organic compounds in the hygroscopic aqueous solution are crucial for thread function. They attract atmospheric water, ensuring that both the axial lines and glycoprotein remain hydrated (Opell et al., 2011a, 2013). This maintains axial line supercontraction (Work, 1981; Work and Morosoff, 1982; Shao and Vollrath, 1999; Shao et al., 1999) and glycoprotein extensibility (Sahni et al., 2011; Opell et al., 2013). These compounds also solvate glycoproteins, enhancing their interactions with surfaces that a thread contacts (Sahni et al., 2014). A number of compounds within the aqueous material have been characterized (Townley and Tillinghast, 2013). Small inorganic compounds make up only 10–20% of a viscous thread's dry mass, with low molecular mass organic compounds (LMMC) comprising 40–70% (Fischer and Brander, 1960; Anderson and Tillinghast, 1980; Tillinghast and Christenson, 1984; Townley et al., 1991).

Spider thread adhesion has been characterized in two ways: the maximum force registered just before thread pull-off (e.g. Opell and

Department of Biological Sciences, Virginia Tech, Blacksburg, VA 24061, USA.

\*Author for correspondence (sstellw@vt.edu)

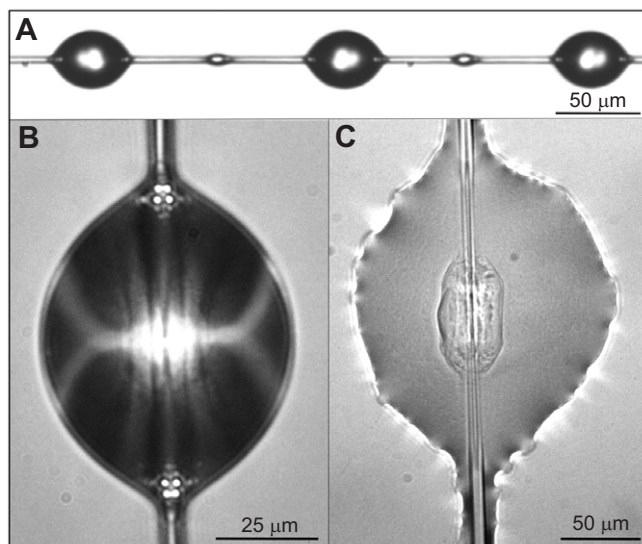


**Fig. 1. Viscous capture thread and droplets.** *Micrathena gracilis* capture thread and droplets (A), and a single suspended (B) and flattened (C) droplet of *Argiope aurantia* as viewed with epi-illumination. The outer aqueous layer and inner glycoprotein core are distinct when a droplet is flattened on a glass slide.

Hendricks, 2009) and the cumulative energy (work) require to pull a thread from a surface (e.g. Sahni et al., 2011). Each index relies on the observation that adhesive forces of multiple droplets are summed as axial lines and droplets elongate under a load, much like the main cable and vertical suspenders effectively bear the load of a suspension bridge deck (Opell and Hendricks, 2007, 2009). Consequently, even a modest degradation in performance at the level of individual droplets can result in a large loss of adhesion and energy dissipation as capture threads resist the struggles of an insect. By examining how droplets respond to UVR, we can understand the broader consequences of this potentially damaging environmental factor on the web's adhesive delivery system.

Two environmental factors are known to affect the capture spiral's glycoprotein: relative humidity (RH; Sahni et al., 2011; Opell et al., 2011a) and temperature (Stellwagen et al., 2014). Depending on the species, extensibility (how far a droplet stretches) and adhesion (the energy required to pull a droplet from a surface) of the glue may continue to increase as RH approaches 100% [*Neoscona crucifera* (Lucas 1839); Opell et al., 2013], or may function optimally at intermediate levels (55% RH in *A. aurantia* and *Larinioides cornutus*; Sahni et al., 2011; Opell et al., 2013) and decrease at lower and higher humidity. Temperature affects the adhesive's viscosity, stiffening the glycoprotein when ambient conditions are cooler and reducing viscosity as temperature increases (Stellwagen et al., 2014). For species like *A. aurantia* that live in exposed habitats, this helps offset the effects of daily humidity oscillations, as low humidity, which increases viscosity, occurs at times of highest temperatures, which have the opposite effect.

The effect of UVR, a third and potentially important environmental factor, on the extensibility of viscous droplets has not been examined. As some webs are exposed to full ambient UVR throughout the course of a day, it is possible that the most damaging component, ultraviolet B radiation (UVB, 280–315 nm), also affects droplet performance. Silkworm silk breaking extensibility is reduced by 67% and work is reduced by 87% after just 1 h of exposure to a combination of UVA and UVB (Aksakal et al., 2015); however, this silk was treated to remove its sericin, a protective,

amorphous, antioxidant glycoprotein. Sericin has been shown to block UVR damage in human (Dash et al., 2008) and mouse (Zhaorigetu et al., 2003) keratinocytes and suppress colon carcinogenesis when fed to mice (Sasaki et al., 2000). Historically considered a waste byproduct from silk manufacturing, sericin is now being used in a wide range of applications, including fabrics, biomedicine and cosmetics (Zhang, 2002). It may be that compounds in the aqueous coating of the viscous droplets of orb weavers' sticky silk spiral also function to protect the glycoprotein glue from direct or oxidative stress.

Alternatively, droplet performance may improve after exposure to UVR, as UVR induces cross-linking in proteins (Bhat and Karim, 2009; Hu et al., 2013). Non-adhesive spider silk continues to improve mechanically after several hours of natural UVA exposure and at twice the natural UVB exposure; however, longer exposures eventually result in degradation (Osaki, 2004; Osaki and Osaki, 2011). Low UV doses may enhance silk performance by further aligning proteins, similar to the 'improvement phase', where molecule alignment is hypothesized to continue after a silk strand is extruded (Agnarsson et al., 2008). Our study included both dark aging and UVB exposure treatments, allowing us to separate and quantify these two effects on the performance of the viscous glue droplets.

Unlike *A. aurantia*, many orb web spider species, including *Leucauge venusta* (Walckenaer 1841) and *Verrucosa arenata* (Walckenaer 1841), build webs in partially shaded areas (Zschokke et al., 2006; Bradley and Hickman, 2009), and others, like *Micrathena gracilis* (Walckenaer 1805), prefer to construct their webs in shaded woody habitats where only an occasional sun fleck strikes their web (Biere and Uetz, 1981). Nocturnal species like *N. crucifera* construct their webs a few hours after dusk (Adams, 2000). By investigating the effects of UVB radiation on the viscous glue droplets of these five araneoid orb-weavers (all of them members of the family Araneidae, except *L. venusta*, which is a member of the family Tetragnathidae), we tested the hypothesis that species which build their webs in open, sunny habitats produce droplets that are less susceptible to UVB damage than those which build their webs in more heavily shaded habitats or at night. We did this by measuring the duration of droplet extension and the angle of axial line deflection produced by extending droplets from fresh threads collected in the early morning (or evening in the case of *N. crucifera*) and compared these with measurements from droplets that were aged in the dark, droplets that were exposed for up to 4 h to UVB levels typical of midday summer sun, and droplets that received approximately three times this amount of UVB exposure.

We also photographed each thread droplet prior to extension, which permitted us to compare the effect of UVB on droplet volume. This is a critical part of the study, as LMMC in a droplet's aqueous layer are responsible for the droplet's hygroscopicity, and a droplet's water content affects glycoprotein extensibility (Opell et al., 2013). Inorganic compounds within the aqueous material are probably not susceptible to UVB damage, but the same may not be true for some of the LMMC. Thus, we also tested the hypothesis that UVB exposure affects the droplet volume of one or more study species.

## RESULTS

UVB exposure had no clear or systematic effect on droplet volume (Table 1). The only treatment differences we observed were for *L. venusta* (1 h UVB, mean±s.d. 1386.0±748 μm<sup>3</sup>; 3 h UVB, 1237.1±435.7 μm<sup>3</sup>; 4 h dark, 1591.2±803.3 μm<sup>3</sup>) and *V. arenata* (1 h UVB, 9472.4±4684.9 μm<sup>3</sup>; 4 h dark, 9584.5±4244.4 μm<sup>3</sup>),

**Table 1. Dimensions of suspended droplets for all species and treatment groups**

	Length ( $\mu\text{m}$ )	Width ( $\mu\text{m}$ )	Volume ( $\mu\text{m}^3$ )	Matched pair (volume)
<i>Argiope aurantia</i>				
Fresh	69.8 $\pm$ 9.7	52.4 $\pm$ 7.9	85,409.4 $\pm$ 37,734.7	
Dark	68.9 $\pm$ 13.5	54.2 $\pm$ 10.3	92,922.9 $\pm$ 46,753.4	$P \geq 0.0974$
Normal UVB	68.0 $\pm$ 12.6	53.1 $\pm$ 10.2	89,481.4 $\pm$ 48,948.9	$P \geq 0.3362$
Extreme UVB	65.0 $\pm$ 11.9	51.4 $\pm$ 9.4	79,265.5 $\pm$ 40,847.8	$P = 0.7462$
<i>Leucage venusta</i>				
Fresh	14.8 $\pm$ 2.0	12.6 $\pm$ 1.3	1030.0 $\pm$ 345.3	
Dark	15.4 $\pm$ 3.1	13.4 $\pm$ 2.8	1342.0 $\pm$ 859.2	$P \geq 0.0043$ (4)
Normal UVB	15.1 $\pm$ 2.5	13.4 $\pm$ 2.2	1257.6 $\pm$ 608.3	$P \geq 0.0262$ , <b>0.0262</b> (1, 3)
Extreme UVB	14.8 $\pm$ 2.7	13.2 $\pm$ 2.3	1207.5 $\pm$ 664.8	$P = 0.3121$
<i>Verrucosa arenata</i>				
Fresh	29.4 $\pm$ 4.1	24.6 $\pm$ 3.6	8037.3 $\pm$ 3787.2	
Dark	30.3 $\pm$ 5.0	25.6 $\pm$ 3.8	9013.2 $\pm$ 4410.4	$P \geq 0.0258$ (4)
Normal UVB	30.4 $\pm$ 4.3	25.7 $\pm$ 3.5	9128.0 $\pm$ 3800.2	$P \geq 0.0237$ (1)
Extreme UVB	30.5 $\pm$ 4.6	25.9 $\pm$ 4.0	9214.9 $\pm$ 4139.6	$P = 0.1403$
<i>Micrathena gracilis</i>				
Fresh	29.0 $\pm$ 3.3	24.2 $\pm$ 2.8	7429.2 $\pm$ 2852.6	
Dark	28.9 $\pm$ 3.9	24.5 $\pm$ 3.4	7725.4 $\pm$ 3419.5	$P \geq 0.1827$
Normal UVB	28.9 $\pm$ 3.6	24.5 $\pm$ 3.2	7688.4 $\pm$ 3048.8	$P \geq 0.1320$
Extreme UVB	27.5 $\pm$ 2.9	23.0 $\pm$ 2.7	6438.3 $\pm$ 2169.3	$P = 0.8763$
<i>Neoscona crucifera</i>				
Fresh	32.6 $\pm$ 9.6	24.0 $\pm$ 7.3	10,070.0 $\pm$ 8452.2	
Dark	31.3 $\pm$ 9.8	22.8 $\pm$ 7.2	8815.2 $\pm$ 6337.2	$P = 0.3682$
Extreme UVB	31.1 $\pm$ 9.4	22.3 $\pm$ 6.5	7992.8 $\pm$ 5650.0	$P = 0.2828$

Significant  $P$ -values ( $<0.05$ ) are in bold. Data for the 'normal UVB' and 'dark' treatments are means obtained by averaging four, 1 h incremental treatment means (due to limited resolution). Individual comparisons were performed for these hourly treatments, and  $P$ -values presented are the lowest of the four comparisons; values in parentheses indicate which of the four hourly comparisons was significantly different from the 'fresh' thread values, if applicable.

where droplet volumes exceeded those of fresh threads. There were no differences for the other hourly treatments, or the extreme treatment for these species.

We brought individual suspended droplets in contact with a probe, then withdrew the probe at a constant rate, and compared the time a thread was under tension while a droplet extended (Fig. 2). The extension times reported in Table 2 provide an index of the extensibility of the glycoprotein within droplets. The hourly UVB irradiated and dark treatments for diurnal species are each presented as an average of the four, 1 h time interval means, as there was no statistical difference between these intervals;  $P$ -values for these combined averages represent the lowest value of the four comparisons. In the full sun species, *A. aurantia*, and partially shaded species, *L. venusta* and *V. arenata*, there were few effects of experimental treatments, and the instances of significance did not form a pattern that we considered

meaningful. For example, the total loaded time (TLT, the time during which deflection of the axial line indicated tension on a droplet prior to and during extension) for *A. aurantia* after the 2 h dark treatment was shorter than that of fresh threads (mean 27.1 $\pm$ 8.4 s). However, no differences were seen for the 3 or 4 h dark treatments, or for any of the normal UVB hourly or extreme treatments. In contrast, for both *M. gracilis* and *N. crucifera*, extreme UVB exposure decreased both TLT and the droplet extension phase (DE), the portion of TLT during which the droplet stretched. In *M. gracilis* there was a 7.1 s (20%) reduction in TLT and a 7.3 s (68%) reduction in DE. *Neoscona crucifera* showed an 11.8 s (23%) decrease in TLT and a 9.7 s (37%) decrease in DE, while the pre-extension phase (PE) that preceded droplet extension remained relatively stable. Both TLT and DE were significantly shorter for *M. gracilis* after exposure to 3 h UVB (Table 3), and DE was significantly shorter after 3 h dark treatment. However, no differences were found after 4 h of normal UVB or dark treatments.

Axial line deflection angles (Fig. 2; supplementary material Table S1) are an estimation of the force on droplets and were measured just prior to droplet extension (0% DE) and at 25%, 50%, 75% and 99% of DE. By combining these angles with values for the diameter and Young's modulus of each species' paired axial lines, we computed the force on an extending droplet (Tables 4, 5). Moderate (1 h) normal UVB exposure increased the force on extending *A. aurantia* droplets, although extreme exposure had a lesser and insignificant effect. This trend was also observed in *L. venusta*, where 3 h normal UVB and 2 h dark treatments increased the force on extending droplets. In contrast, for *M. gracilis*, both 3 h normal and extreme UVB treatments progressively decreased the force during the 50–99% extension intervals, with extreme exposure having an average of 2.5 times the effect of the mean hourly exposure values. During the 50–99% intervals, the dark treatment reduced the force on *N. crucifera* droplets, and the extreme

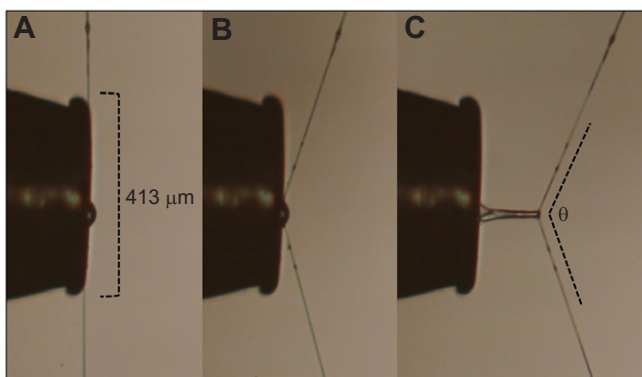


**Fig. 2. Droplet extension configurations.** Droplet in the unloaded (A), pre-extension (B) and extension (C) phases. Angular deflection of the support line corresponds to the force on droplets in pre-extension and extension phases.

**Table 2. Extension phase times for all species and treatments**

	TLT (s)	Matched pair TLT	PE (s)	Matched pair PE	DE (s)	Matched pair DE
<i>A. aurantia</i>						
Fresh	30.7±8.5		17.6±6.4		13.1±6.9	
Dark	29.5±8.9	<b><math>P \geq 0.0243</math> (2)</b>	17.4±7.5	$P \geq 0.5492$	11.8±4.5	$P \geq 0.1088$
Normal UVB	30.4±10.5	$P \geq 0.4645$	17.0±9.0	$P \geq 0.2539$	13.4±5.5	$P \geq 0.8561$
Extreme UVB	32.1±7.7	$P = 0.6780$	15.1±7.2	$P = 0.1856$	17.0±6.3	$P = 0.0781$
<i>L. venusta</i>						
Fresh	31.0±7.6		24.9±7.8		6.1±3.4	
Dark	36.5±8.2	<b><math>P \geq 0.0331</math> (2)</b>	28.6±7.4	$P \geq 0.1828$	7.9±5.2	$P \geq 0.1396$
Normal UVB	33.6±7.2	<b><math>P \geq 0.0463</math> (3)</b>	26.6±6.2	<b><math>P \geq 0.0352</math> (3)</b>	7.0±5.3	$P \geq 0.2748$
Extreme UVB	30.3±5.8	$P = 0.7980$	25.3±5.1	$P = 0.8805$	5.0±2.6	$P = 0.3600$
<i>V. arenata</i>						
Fresh	22.1±7.5		12.0±2.9		10.1±5.1	
Dark	21.1±6.7	$P \geq 0.4037$	12.3±3.7	$P \geq 0.4037$	8.8±4.1	$P \geq 0.1375$
Normal UVB	22.2±3.3	$P \geq 0.4743$	13.0±1.9	$P \geq 0.1161$	9.2±2.2	$P \geq 0.3272$
Extreme UVB	22.9±6.1	$P = 0.7786$	13.3±2.3	$P = 0.8257$	9.6±5.0	$P = 0.4143$
<i>M. gracilis</i>						
Fresh	36.3±8.3		25.6±6.7		10.7±6.0	
Dark	32.5±8.5	$P \geq 0.0557$	25.7±6.9	$P \geq 0.2024$	6.7±5.6	<b><math>P \geq 0.0413</math> (3)</b>
Normal UVB	33.9±8.4	<b><math>P \geq 0.0209</math> (3)</b>	26.2±7.7	$P \geq 0.1691$	7.7±5.2	<b><math>P \geq 0.0397</math> (3)</b>
Extreme UVB	29.2±5.1	<b><math>P = 0.0011</math></b>	25.8±5.3	$P = 0.9698$	3.4±3.2	<b><math>P = 0.0087</math></b>
<i>N. crucifera</i>						
Fresh	51.8±13.4		25.4±7.3		26.3±11.3	
Dark	45.7±17.9	$P = 0.1803$	21.4±6.5	$P = 0.0892$	24.3±15.5	$P = 0.5325$
Extreme UVB	40.5±18.1	<b><math>P = 0.0061</math></b>	23.9±9.1	$P = 0.4551$	16.6±13.7	<b><math>P = 0.0024</math></b>

TLT, total loaded time; PE, pre-extension phase; DE, droplet extension phase.

Data are means±s.d. Significant  $P$ -values ( $<0.05$ ) are in bold. Data for the 'normal UVB' and 'dark' treatments are means obtained by averaging four, 1 h incremental treatment means (due to limited resolution). Individual comparisons were performed for these hourly treatments, and  $P$ -values presented are the lowest of the four comparisons; values in parentheses indicate which of the four hourly comparisons was significantly different from the 'fresh' thread values, if applicable.

treatment reduced the force during the 50–99% intervals by an average of 23%, although this difference was not significant.

When the force on an extending droplet is plotted against extension time (Fig. 3), interspecific differences in droplet response to aging and UVB exposure appear. Extreme and combined hourly normal UVB exposures increased the force registered by extending *A. aurantia* droplets more than did the combined hourly dark treatments. Force on *L. venusta* droplets increased after both dark and UVB hourly treatments, but was little affected by the extreme UVB treatment. Neither aging nor UVB exposure had an effect on the performance of *V. arenata* droplets. However, extreme UVB greatly reduced the force

registered by *M. gracilis* and slightly reduced that registered by *N. crucifera* droplets. Extreme UVB lengthened the extension times of *A. aurantia* droplets, but reduced the extension times of the other species.

The area under each of the force–extension time curves represents relative toughness and is an index of the energy required to extend a droplet (Fig. 3). The energy absorbed by *L. venusta* increased after 1 h dark (111%,  $P = 0.0440$ ) and remained higher after 2 h dark (114%,  $P = 0.0272$ ). *Verrucosa arenata* droplets remained remarkably stable, while energy absorption by *M. gracilis* droplets declined following normal UVB exposure, being reduced by 58% ( $P = 0.0107$ ) after 3 h UVB and 76% ( $P = 0.0205$ ) after

**Table 3. *Micrathena gracilis* extension phase times for all treatments**

	TLT (s)	Matched pair TLT	PE (s)	Matched pair PE	DE (s)	Matched pair DE
Fresh	36.3±8.3		25.6±6.7		10.7±6.0	
Dark						
1 h	30.9±8.1	$P = 0.0845$	22.7±3.7	$P = 0.2024$	8.2±7.3	$P = 0.3628$
2 h	31.7±8.7	$P = 0.2088$	25.7±8.2	$P = 0.9896$	6.0±4.8	$P = 0.0557$
3 h	31.5±7.2	$P = 0.0557$	25.4±5.5	$P = 0.8962$	6.1±3.8	<b><math>P = 0.0431</math></b>
4 h	35.7±10.0	$P = 0.8411$	29.1±8.2	$P = 0.3028$	6.6±6.2	$P = 0.1219$
Normal UVB						
1 h	32.8±7.5	$P = 0.3411$	24.0±5.7	$P = 0.5666$	8.7±4.8	$P = 0.3879$
2 h	35.9±9.2	$P = 0.9025$	27.3±9.4	$P = 0.6117$	8.6±6.0	$P = 0.3095$
3 h	30.0±8.4	<b><math>P = 0.0209</math></b>	23.5±6.2	$P = 0.2950$	6.5±4.3	<b><math>P = 0.0397</math></b>
4 h	36.8±7.9	$P = 0.8883$	29.8±8.2	$P = 0.9698$	7.0±5.7	$P = 0.1659$
Extreme UVB	29.2±5.1	<b><math>P = 0.0011</math></b>	25.8±5.3	$P = 0.9698$	3.4±3.2	<b><math>P = 0.0087</math></b>

Data are means±s.d. Significant  $P$ -values ( $<0.05$ ) are in bold.

Table 4. Force calculations at 0%, 25%, 50%, 75% and 99% of the droplet extension time for all species and treatment groups

	Force 0% ( $\mu$ N)	Matched pair 0%	Force 25% ( $\mu$ N)	Matched pair 25%	Force 50% ( $\mu$ N)	Matched pair 50%	Force 75% ( $\mu$ N)	Matched pair 75%	Force 99% ( $\mu$ N)	Matched pair 99%
<i>A. aurantia</i>										
Fresh	28.7 $\pm$ 25.5		14.4 $\pm$ 19.2		11.2 $\pm$ 20.5		7.8 $\pm$ 21.9		6.8 $\pm$ 22.9	
Dark	30.1 $\pm$ 31.6	$P\geq 0.6585$	23.2 $\pm$ 34.8	$P\geq 0.0944$	18.1 $\pm$ 36.1	$P\geq 0.1774$	14.9 $\pm$ 33.4	$P\geq 0.1007$	9.4 $\pm$ 28.8	$P\geq 0.2626$
Normal	31.1 $\pm$ 36.0	$P\geq 0.3770$	26.0 $\pm$ 38.9	<b><math>P\geq 0.0090</math> (1)</b>	24.6 $\pm$ 43.7	<b><math>P\geq 0.0312</math> (1)</b>	19.6 $\pm$ 40.2	<b><math>P\geq 0.0346</math> (1)</b>	10.5 $\pm$ 31.1	<b><math>P\geq 0.0134</math> (1)</b>
UVB										
Extreme	22.3 $\pm$ 25.2	$P=0.2709$	19.3 $\pm$ 27.7	$P=0.3481$	19.7 $\pm$ 33.7	$P=0.1667$	20.3 $\pm$ 37.3	$P=0.1054$	11.4 $\pm$ 26.8	$P=0.1800$
UVB										
<i>L. venusta</i>										
Fresh	13.6 $\pm$ 9.4		13.7 $\pm$ 9.3		14.5 $\pm$ 9.1		14.7 $\pm$ 8.7		14.8 $\pm$ 8.6	
Dark	18.1 $\pm$ 9.8	$P\geq 0.1036$	19.2 $\pm$ 10.0	<b><math>P\geq 0.0437</math> (2)</b>	21.1 $\pm$ 10.5	<b><math>P\geq 0.0246</math> (2)</b>	22.9 $\pm$ 10.9	<b><math>P\geq 0.0064</math> (2)</b>	24.4 $\pm$ 11.5	<b><math>P\geq 0.0066</math> (2)</b>
Normal	15.9 $\pm$ 7.4	$P\geq 0.0530$	16.9 $\pm$ 7.5	<b><math>P\geq 0.0271</math> (3)</b>	18.1 $\pm$ 7.9	<b><math>P\geq 0.0243</math> (3)</b>	19.7 $\pm$ 8.6	<b><math>P\geq 0.0212</math> (3)</b>	20.5 $\pm$ 9.5	<b><math>P\geq 0.0226</math> (3)</b>
UVB										
Extreme	14.1 $\pm$ 5.9	$P=0.8661$	14.5 $\pm$ 6.2	$P=0.7884$	15.0 $\pm$ 6.4	$P=0.8406$	15.6 $\pm$ 6.9	$P=0.7593$	16.2 $\pm$ 7.2	$P=0.6406$
UVB										
<i>V. arenata</i>										
Fresh	13.4 $\pm$ 8.1		18.4 $\pm$ 11.8		26.3 $\pm$ 17.0		33.3 $\pm$ 22.8		37.3 $\pm$ 28.4	
Dark	12.5 $\pm$ 8.6	$P\geq 0.5983$	17.2 $\pm$ 11.4	$P\geq 0.5257$	22.9 $\pm$ 15.2	$P\geq 0.2967$	28.3 $\pm$ 19.3	$P\geq 0.2485$	31.2 $\pm$ 22.9	$P\geq 0.2329$
Normal	15.1 $\pm$ 8.6	$P\geq 0.0969$	20.3 $\pm$ 11.4	$P\geq 0.1448$	26.5 $\pm$ 15.2	$P\geq 0.2661$	32.6 $\pm$ 19.2	$P\geq 0.2329$	35.1 $\pm$ 21.8	$P\geq 0.2419$
UVB										
Extreme	14.7 $\pm$ 6.9	$P=0.5402$	20.1 $\pm$ 10.1	$P=0.6213$	26.5 $\pm$ 14.8	$P=0.7967$	32.6 $\pm$ 19.7	$P=0.9208$	35.0 $\pm$ 22.9	$P=0.9782$
UVB										
<i>M. gracilis</i>										
Fresh	27.6 $\pm$ 14.7		25.0 $\pm$ 15.2		26.7 $\pm$ 14.9		28.3 $\pm$ 15.0		27.7 $\pm$ 15.7	
Dark	28.8 $\pm$ 14.2	$P\geq 0.2409$	24.7 $\pm$ 13.9	$P\geq 0.2193$	25.1 $\pm$ 14.8	$P\geq 0.1836$	25.4 $\pm$ 15.5	$P\geq 0.0791$	23.0 $\pm$ 16.0	<b><math>P\geq 0.0284</math> (3)</b>
Normal	30.0 $\pm$ 17.4	$P\geq 0.1460$	23.9 $\pm$ 15.1	$P\geq 0.0673$	23.3 $\pm$ 15.2	<b><math>P\geq 0.0156</math> (3)</b>	23.1 $\pm$ 15.4	<b><math>P\geq 0.0075</math> (3)</b>	20.6 $\pm$ 15.2	<b><math>P\geq 0.0048</math> (3)</b>
UVB										
Extreme	26.2 $\pm$ 11.0	$P=0.6118$	19.2 $\pm$ 9.6	$P=0.0961$	17.9 $\pm$ 9.6	<b><math>P=0.0357</math></b>	17.0 $\pm$ 9.5	<b><math>P=0.0240</math></b>	14.5 $\pm$ 8.8	<b><math>P=0.0177</math></b>
UVB										
<i>N. crucifera</i>										
Fresh	26.2 $\pm$ 15.9		32.1 $\pm$ 17.5		41.7 $\pm$ 20.8		50.5 $\pm$ 24.3		56.8 $\pm$ 27.5	
Dark	18.8 $\pm$ 15.3	$P=0.1369$	20.9 $\pm$ 16.4	$P=0.0594$	27.9 $\pm$ 19.7	<b><math>P=0.0395</math></b>	34.4 $\pm$ 24.1	<b><math>P=0.0411</math></b>	38.1 $\pm$ 26.3	<b><math>P=0.0254</math></b>
Extreme	27.0 $\pm$ 21.8	$P=0.8556$	28.0 $\pm$ 21.4	$P=0.3889$	33.2 $\pm$ 23.0	$P=0.1360$	38.8 $\pm$ 25.1	$P=0.0845$	41.9 $\pm$ 26.3	$P=0.0516$
UVB										

Data are means $\pm$ s.d. Significant  $P$ -values ( $<0.05$ ) are in bold. Data for the 'normal UVB' and 'dark' treatments are means obtained by averaging four, 1 h incremental treatment means (due to limited resolution). Individual comparisons were performed for these hourly treatments, and  $P$ -values presented are the lowest of the four comparisons; values in parentheses indicate which of the four hourly comparisons was significantly different from the 'fresh' thread values, if applicable.

Table 5. Young's moduli used in the force calculations for each species

	Axial fiber diameter (μm)	Young's modulus (GPa)
<i>Argiope aurantia</i>	4.8±1.50	0.009±0.011
<i>Leucauge venusta</i>	0.9±0.26	0.058±0.046
<i>Verrucosa arenata</i>	1.5±0.64	0.098±0.199
<i>Micrathena gracilis</i>	1.3±0.30	0.052±0.053
<i>Neoscona crucifera</i>	3.0±1.18	0.010±0.005

Data were taken from supplementary table 4 in Sensenig et al., 2010.

extreme UVB. *Neoscona crucifera* droplets exhibited a 45% reduction ( $P=0.0251$ ) in energy absorption after the extreme UVB treatment.

DISCUSSION

The viscous capture spiral threads of orb-weaving spiders have been selected to retain insects that have intercepted a web (Blackledge and Eliason, 2007). This allows a spider time to locate prey in the web, evaluate the risk associated with its capture and, finally,

subdue it. As a viscous thread sums the adhesion of an estimated 20 droplets via the suspension bridge mechanism (Opell and Hendricks, 2007, 2009), small changes in individual droplet performance can have a large impact on thread performance. A decrease of even a few seconds in prey retention time can mean a lost feeding opportunity for an orb-weaving spider (Blackledge and Zevenbergen, 2006). Moreover, the ability of the droplets to absorb the energy of struggling prey is crucial, and can be affected by environmental conditions such as humidity (Sahni et al., 2011; Opell et al., 2011a, 2013) and temperature (Stellwagen et al., 2014). This study demonstrated that, as hypothesized, the droplets of five spider species that ranged from full sun to nocturnal habitats were differentially affected by exposure to UVB radiation.

As gauged by droplet volume, UVB does not appear to impact the LMMC in droplets, supporting another observation that these compounds resist degradation (Opell et al., 2015). Therefore, as all observations were made under the same humidity, any differences in droplet performance can be attributed to the direct effect of UVB on glycoprotein structure and not to changes in glycoprotein

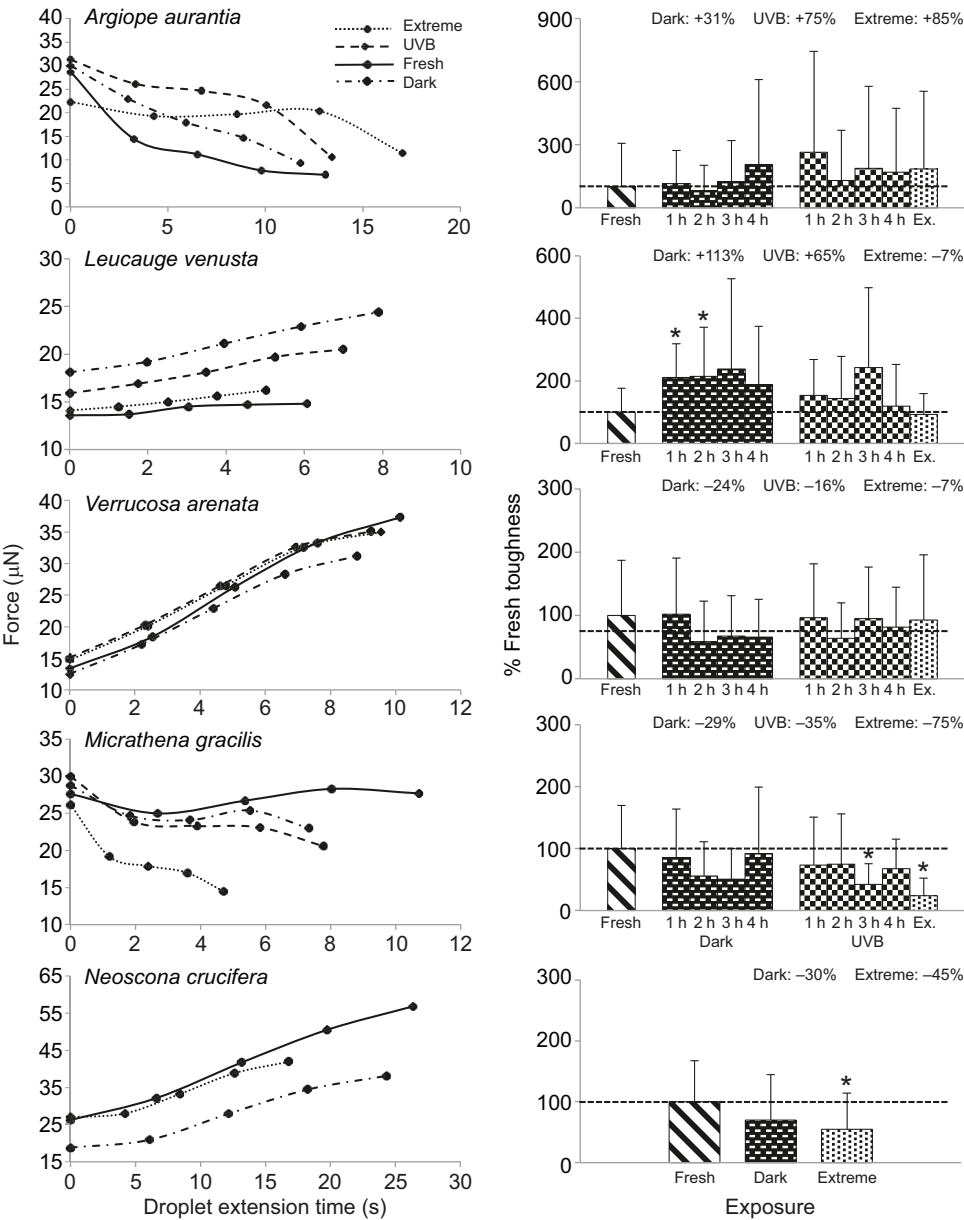


Fig. 3. Force–extension time plots for viscous droplets and corresponding histograms of relative toughness for droplets in each treatment. Points in the force–extension time plots are mean values and are connected by smoothed lines. Relative toughness values, determined from the area under the force–time curves, are means±s.d., with each significant difference from fresh threads, as determined by matched pair *t*-tests, being indicated by an asterisk. Dashed lines indicate the level of relative toughness for the fresh threads (for easy visual comparison).

hydration mediated by LMMC. These LMMC also contribute more directly to thread adhesion by solvating and softening glycoproteins, and thus facilitate glycoprotein–surface interactions (Sahni et al., 2014). Therefore, the stability of droplet volume suggests that droplet adhesion was also unaffected by UVB exposure.

The viscous droplets of all five species continued to extend even after extreme UVB exposure, although only the performance of *V. arenata* droplets was wholly unaffected by aging or UVB irradiation. Droplets of *M. gracilis*, which are found within forests, and those of the nocturnal *N. crucifera*, exhibited significant reductions in performance after exposure to extreme UVB, with the relative toughness of the former dropping by three-quarters and of the latter by almost half (Fig. 3). Interestingly, the droplets of *M. gracilis* showed a reduction in both force and extension time, whereas those of *N. crucifera* maintained a similar force to fresh threads, but were reduced exclusively in extension time. Thus, our observations support the hypothesis that the glycoprotein within viscous droplets produced by shade-dwelling and nocturnal species is more susceptible to UVB damage than that produced by species that live in exposed habitats. In contrast, normal and extreme UVB exposure increased the relative toughness of *A. aurantia*, a species found in exposed habitats, by increasing the force on extending droplets after normal UVB exposure, and increasing both force and the duration of droplet extension after extreme exposure. The relative toughness of *L. venusta* droplets, a species preferring partial shade, increased nearly twice as much during the dark treatment as during normal UVB treatment, while being little affected by extreme UVB. This suggests that the performance of *L. venusta* droplets is enhanced by a post-production improvement phase (Agnarsson et al., 2008) and that UVB exposure interferes with or reverses these changes. Additionally, *L. venusta* is a member of the family Tetragnathidae, while all other species used in this study are in the family Araneidae, suggesting phylogenetic differences in glue properties.

Although *N. crucifera* is a nocturnal species, extreme UVB exposure reduced the toughness of its droplets 30% less than it did those of the diurnal species *M. gracilis*. Though unexpected, this may be explained by observations that *Neoscona* species leave their webs up during the day, switching from a night-time monitoring position at the web's hub to a cryptic daytime position in vegetation adjacent to the web (Edwards, 1984). Their forest edge habitat would, thus, leave the webs exposed to UVB, which may explain their higher resistance to UVB than those of *M. gracilis*, whose webs are rarely exposed to even brief specks of sunlight. By collecting *N. crucifera* web samples in the evening and measuring them the following day, our procedures allowed for at least 10 h of post-production curing of their threads before our treatments began, making it surprising that further aging during our tests had an apparent, though not a statistically significant, effect.

UVB irradiation mechanically strengthens the dragline silk of several diurnal spider species (Osaki, 2004; Osaki and Osaki, 2011), although the mechanism of change is undocumented. UVB irradiation also increases the viscosity of proteinaceous fish gelatin (Otoni et al., 2012), where it is thought that UVB produces free radicals, which link the aromatic compounds in these materials (Fujimori, 1965). The capture spiral glycoprotein of *Araneus diadematus* includes aromatic amino acids (Andersen, 1970), suggesting that this may contribute to the increased toughness of droplets observed for *A. aurantia* following UVB exposure. However, this information is lacking for the species we studied, making it difficult to assess whether levels of these

aromatic compounds could be responsible for the observed differences.

Thread performance data exhibited high variance and although matched pair statistics reduced the impact of this variance, it made analysis challenging and probably accounts for such anomalies as the *M. gracilis* TLT fresh value differing from 3 h but not from 4 h UVB exposure values. The source of this inter-individual variance may lie in size, nutritional or reproductive status differences among the mature females that produced the threads we studied. All the webs from which threads were collected appeared normal and did not show signs of spider senescence that has been reported for some orb-weavers (Eberhard, 1971). Differences in temperature and humidity at the time of web construction or thread position in the web may also affect droplets. However, we attempted to account for these issues by controlling room conditions and using threads from the outer 30% of a web.

Our study adds UVB irradiation to the list of factors known to affect the performance of spider glycoprotein glue, which includes humidity (Opell et al., 2011a, 2013), temperature (Stellwagen et al., 2014) and strain rate (Sahni et al., 2011). It is important to more fully understand these effects as material science moves toward producing environmentally non-toxic and energy conservative adhesives inspired by spider thread glycoprotein. Interspecific differences in the performance of viscous droplets in response to both humidity and UVB exposure offer a preview of the range of adhesives that might be modeled after orb spider glycoprotein glue. This glue is produced at ambient temperatures, is robust yet biodegradable and, as this research demonstrates, can be very resistant to damaging UVB. In addition, this glue does not need the additional glandular processing of structural dragline silk, a requirement that has been the major obstruction to making synthetic silks on a commercial scale. Thus, a biomaterial modeled on spider glue may be both easier to produce and, through an understanding of the molecular differences that adapt the glue of different species to their habitats, easier to engineer for a range of applications.

## MATERIALS AND METHODS

### Study species and thread collection

Thread samples were collected from webs constructed by individual adult females of *A. aurantia* ( $N=13$ ), *L. venusta* ( $N=12$ ), *V. arenata* ( $N=12$ ) and *M. gracilis* ( $N=12$ ) on and near the Virginia Tech campus in Blacksburg, Montgomery County, VA, USA, from 9 August to 28 September 2013. Each sample was collected between 05:30 h and 08:30 h and all images and videos were captured by 16:00 h the same day. *Neoscona crucifera* ( $N=11$ ) thread samples were collected from 21 August to 31 August 2014 between 21:30 h and 23:00 h and their study was completed by 16:00 h on the following day. Webs from *N. crucifera* were exposed to only the extreme treatment, as hourly data from the diurnal species, collected in the previous year, did not appear useful in resolving the effects of short-term, low-level UVB exposure. A sector of each spider's web was collected on either a 15×52 cm aluminium rectangular frame or a 17 cm diameter aluminium ring with a bar across its center. The upper surfaces of these frames and rings were covered with Scotch® double-sided tissue tape (Tape 410M, 3M, St Paul, MN, USA), which adhered to web sectors, maintaining the threads at their native tension. Threads extending from the collecting frame were cut with a scissor to avoid distorting the sample when the frame was withdrawn from the web. We placed web-sampling frames in closed containers for transport to the laboratory. The location of each sampled web was marked with flagging tape to ensure that threads from an individual spider's web were included only once in the study.

To stabilize webs before transferring thread strands to microscope sampler slides, we placed 4 mm wide brass bars that were covered with double-sided carbon tape (product 77816, Electron Microscopy Sciences,

Hatfield, PA, USA) across the frame's rim along web radii. This further isolated the web sample and ensured that the tension of viscous threads adjacent to the ones being collected was not altered. We used forceps, which were blocked open to accommodate the separation of the supports on the sampler slide, to collect individual viscous threads and transfer them to a microscope slide sampler. Double-sided carbon tape on both tips of the forceps held each thread strand securely when the thread was pulled or burned free using a hot wire probe. Threads were placed on the tops of a sampler's U-shaped brass struts, which were epoxied at 4.8 mm intervals to microscope slides and covered with double-sided carbon tape (fig. 3 in Opell et al., 2011b).

To ensure that the probe used to extend droplets contacted only a single droplet, we used a minuten insect pin moistened with distilled water to move away droplets that were adjacent to the test droplet located at the center of the thread strand. This process retained the aqueous coating of the strand's axial fibers, as demonstrated by the formation of small droplets similar to those often present between the large primary droplets of many viscous threads. Observations were made at 24°C and 55% RH and were established by turning electric humidifiers on and off, and adjusting the room's thermostat.

### UVB irradiance

A single 14.7 W, 306 nm spectral peak UVB fluorescent tube (G15T8E; 440.4 mm length, 25.4 mm diameter; USHIO Inc., Cypress, CA, USA) was used to irradiate samples. The lamp hung diagonally from the top interior of a white-surfaced ply board cabinet (52.5×37×48 cm). Airflow through the chamber was maintained by a small fan in the top of the chamber that drew air through three 7.5 cm diameter holes in the cabinet's lower sides and back.

We placed microscope slide samplers with threads on a black felt-covered Styrofoam block, which had a central hole to accommodate the sensor of the UVB meter used to measure thread exposure. Two slides with thread samples were placed on either side of a UVB meter sensor probe to provide accurate readings of irradiance and cumulative UVB dosage throughout each trial. Irradiance was measured using a PMA2200 photometer radiometer (Solar Light Co., Inc., Glenside, PA, USA) equipped with a UVB detector (PMA2106-WP, Solar Light Co., Inc.) calibrated traceable to the National Institute of Standards and Technology (NIST) on 29 July 2013 with a spectral sensitivity from 280 to 320 nm, and peak sensitivity ~312 nm by the manufacturer.

To create a dark treatment cylinder for thread sampler slides, we epoxied two 35 mm plastic film development canisters together to create a 21 cm long, 9 cm diameter cylinder with light baffles at either end that permitted air flow. We placed this cylinder on the floor of the chamber at the same height as the platform on which exposed thread samples rested. The dark treatment cylinder and the UV cabinet maintained ambient room temperature and humidity within a standard deviation of ±0.13°C and ±1.3% RH, and 0.08°C and ±1.7% RH, respectively, as recorded every 30 s for 2 h by Hobo® temperature/relative humidity data loggers (model U23-002; Onset Computer Corp., Bourne, MA, USA).

For each of the following 10 treatments, we tested two droplets from an individual's web sample: (1) fresh threads measured immediately after UVB treatments and their controls had begun; (2–5) threads kept in the dark canister within the UVB chamber for 1, 2, 3 and 4 h; (6–9) threads irradiated for 1, 2, 3 and 4 h of light at ~2.5 W m<sup>-2</sup>, a level typical of full sunlight received in this area in late summer from 10:00 h to 14:00 h and established by placing polyethylene plastic filters above the thread samplers; (10) threads exposed to an extreme irradiance for 4 h at ~7.5 W m<sup>-2</sup>, the maximum level produced by the UVB lamp.

### Droplet extension and volume

We photographed each isolated test droplet immediately prior to extension. All observations were made within a chamber that held microscope slide samplers and rested on the mechanical stage of a Mitutoyo FS60 inspection microscope (fig. 4 in Opell et al., 2011a). A steel probe was inserted through a port in the side of the test chamber and its 413 µm wide polished tip, previously cleaned with 95% ethanol on a Kimwipe, was aligned and brought into contact with the focal droplet and anchored to a stable mount. To ensure full droplet adhesion, the probe was pressed against the droplet

until the thread was deflected by a distance of 500 µm. We then recorded a 60 frames s<sup>-1</sup> video as the probe was withdrawn from the droplet at a velocity of 69.6 µm s<sup>-1</sup> by a computer-controlled stepping motor connected to the microscope stage's x-axis by a flexible belt.

We used ImageJ (Rasband 1997–2014) to measure droplet length (DL; dimension parallel to the support line) and droplet width (DW), and from these measurements computed droplet volume (DV) using the formula (Opell and Schwend, 2007; Liao et al., 2015):

$$DV = \frac{2\pi \times DW^2 \times DL}{15}. \quad (1)$$

### Droplet extension and axial line angle deflection

The TLT of droplet extension begins when the axial line is deflected from its initial non-loaded, 180 deg configuration and ends when the droplet returns to a non-loaded condition. We divided TLT into two phases; the pre-extension (PE) phase, during which a droplet exhibited tensile axial line deflection, but did not extend, thus holding the axial line in contact with the probe, and the droplet extension (DE) phase, which began when a droplet filament started to form and ended when the axial line returned to its 180 deg configuration at the end of TLT (fig. 4 in Stellwagen et al., 2014). During DE, we measured five axial line deflection angles using iMovie 11 (Apple Inc., 2010) and ImageJ programs: the angle at the initiation of this filament formation, and the angles at 25%, 50%, 75% and 99% of the total duration time of DE.

### Force calculation

We used the diameter and Young's modulus of each species' axial fibers (Table 5) to estimate the force ( $F_{\text{total}}$ ) on a droplet in three computational steps: (1) determining the extension of the axial lines on either side of an extending droplet, (2) converting this extension to force and (3) summing these force vectors to determine force exerted on a droplet filament (Fig. 4).

Each droplet was located near the center of a 4800 µm long support strand; however, the entire thread was not captured in videos. Therefore, we used the supporting line's central deflection angle to calculate the change in length ( $\Delta L$ ) of each side ( $L_0=2400$  µm) of the support thread according to the following formulas:

$$L = \frac{2400}{\sin(\theta \times 0.5)}, \quad (2)$$

$$\Delta L = L - L_0. \quad (3)$$

Knowing the extensions of either side of the thread that supported a droplet, and the diameters and Young's modulus values for each species' axial fibers, we calculated the force on each stretching thread on either side of a

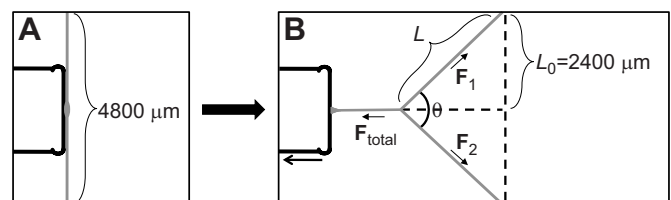


**Fig. 4. Computing force on an extending droplet from support line deflection.** (A) The probe initially contacts the droplet in the center of a 4800 µm long strand of thread, at which point there is no force on the droplet, as indicated by the support line's 180 deg configuration. (B) The droplet has extended as the thread and probe move apart, and the tension on the elongating droplet is visible in the deflection of the support line. Force on the droplet is calculated from the length of one half of a stretching thread ( $L$ ), the original length of that half-thread ( $L_0$ ) and the angle of axial deflection ( $\theta$ ). The force vectors of each side of the stretching thread ( $F_1$ ,  $F_2$ ) are summed to determine the force on a droplet ( $F_{\text{total}}$ ).

droplet ( $F_1$ ,  $F_2$ ) using the formula:

$$F_1, F_2 = \frac{EA_0\Delta L}{L_0}, \quad (4)$$

where  $E$  is Young's modulus and  $A_0$  is two times the instantaneous cross-sectional area of each of a strand's two cylindrical axial fibers. The Young's moduli used in these calculations are appropriate for extensions less than ~50%, after which strain-hardening of the silk alters the properties of the silk (Sensenig et al., 2010). We calculated the average percentage change in length of the threads during droplet extension for each treatment to be substantially less than 50% (supplementary material Table S2). Instantaneous cross-sectional area, which accounts for the narrowing of axial fibers as they are stretched, was determined by multiplying reported cross-sectional area (Table 5) by the ratio of the initial thread length to the final thread length.

To determine the total force exerted on a droplet filament, the angular deflection of a droplet's support line was again used to sum the force vectors of both sides of the support lines of a droplet, using the formula:

$$F_{\text{total}} = 2 \cos(\theta \times 0.5) F_1. \quad (5)$$

Toughness or work is the area under a stress–strain curve, and because we generated stress–seconds of extension curves, we term the area under these curves relative toughness. This index of cumulative force on a droplet as it is extended was therefore equated to the area under a treatment's force–extension time plot (Fig. 3). To approximate this index for each treatment, we summed the products of force and DE at each DE interval (0%, 25%, 50%, 75% and 99%), as described in the following formula, where  $F$  is the total force on an extending droplet and  $I$  is the droplet interval:

$$\frac{(F_I + F_{I+1})}{2} \times (DE_{I+1} - DE_I). \quad (6)$$

## Analysis

We used JMP (SAS Institute, Cary, NC, USA) to analyze data and considered comparisons with  $P \leq 0.05$  as significant. All observations were normally distributed (as confirmed by Shapiro–Wilk  $W$ -tests having  $P \leq 0.05$ ). Each treatment value was compared with the fresh thread value, which served as the control. Droplet size and performance were very similar within an individual web sample but showed some inter-individual difference. To address this, we followed a repeated measures design, comparing values with matched pair  $t$ -tests. This approach results in any bias in the measurement of fresh droplets affecting each comparison. However, our best gauge of similarity of control and treatment droplets is droplet length and width, which were quite similar (Table 1).

## Acknowledgements

Carlyle C. Brewster assisted with statistical analyses.

## Competing interests

The authors declare no competing or financial interests.

## Author contributions

S.D.S. collected and prepared thread samples, performed droplet extensions and image measurements, analyzed data, and prepared the manuscript and figures. B.D.O. designed and constructed the instrumentation used in this study, collected and helped prepare thread samples, and contributed to data analysis, and manuscript and figure preparation. M.E.C. assisted with droplet extension, image measurements, and data entry.

## Funding

Funds from the State Council for Higher Education for Virginia provided the digital camera used in this study. This study was supported by National Science Foundation grant IOS-1257719.

## Supplementary material

Supplementary material available online at <http://jeb.biologists.org/lookup/suppl/doi:10.1242/jeb.123067/-DC1>

## References

- Adams, M. R. (2000). Choosing hunting sites: web site preferences of the orb weaver spider, *Neoscona crucifera*, relative to light cues. *J. Insect Behav.* **13**, 299–305.
- Agnarsson, I., Boutry, C. and Blackledge, T. A. (2008). Spider silk aging: initial improvement in a high performance material followed by slow degradation. *J. Exp. Zool. A Ecol. Genet. Physiol.* **309A**, 494–504.
- Aksakal, B., Koç, K., Yargı, Ö. and Tsohkallo, K. (2015). Effect of UV-light on the uniaxial tensile properties and structure of uncoated and TiO2 coated Bombyx mori silk fibers. *Spectrochim. Acta A Mol. Biomol. Spectrosc.* doi:10.1016/j.saa.2015.01.131
- Andersen, S. O. (1970). Amino acid composition of spider silks. *Comp. Biochem. Physiol.* **35**, 705.
- Anderson, C. M. and Tillinghast, E. K. (1980). GABA and taurine derivatives on the adhesive spiral of the orb web of *Argiope* spiders, and their possible behavioural significance. *Physiol. Entomol.* **5**, 101–106.
- Apstein, C. H. (1889). *Bau und Funktion der Spinnröhren der Araneida*. *Arch. Naturgesch.* Vol. 29. Berlin: Nikolai.
- Bhat, R. and Karim, A. A. (2009). Ultraviolet irradiation improves gel strength of fish gelatin. *Food Chem.* **113**, 1160–1164.
- Biere, J. M. and Uetz, G. W. (1981). Web orientation in the spider *Micrathena gracilis* (Araneae: Araneidae). *Ecology* **62**, 336–344.
- Blackledge, T. A. and Eliason, C. M. (2007). Functionally independent components of prey capture are architecturally constrained in spider orb webs. *Biol. Lett.* **3**, 456–458.
- Blackledge, T. A. and Zevenbergen, J. M. (2006). Mesh width influences prey retention in spider orb webs. *Ethology* **112**, 1194–1201.
- Boys, C. V. (1889). Quartz fibres. *Nature* **40**, 247–251.
- Bradley, R. A. and Hickman, W. L. (2009). Spiders (Araneae) of the Glen Helen Nature Preserve, Green County, OH. *Ohio J. Sci.* **18**, 1–27.
- Carlson, K. M. and Smith, K. C. (1981). Effect of the uvrD3 mutation on ultraviolet radiation-induced DNA-repair replication in *Escherichia coli* K12. *Mutat. Res. Fundam. Mol. Mech. Mutagen.* **84**, 257–262.
- Connelly, S. J., Moeller, R. E., Sanchez, G. and Mitchell, D. L. (2009). Temperature effects on survival and DNA repair in four freshwater cladoceran *Daphnia* species exposed to UV radiation. *Photochem. Photobiol.* **85**, 144–152.
- Dash, R., Mandal, M., Ghosh, S. and Kundu, S. C. (2008). Silk sericin protein of tropical tasar silkworm inhibits UVB-induced apoptosis in human skin keratinocytes. *Mol. Cell. Biochem.* **311**, 111–119.
- Eberhard, W. G. (1971). Senile web patterns in *Uloborus diversus* (Araneae: Uloboridae). *Dev. Psychobiol.* **4**, 249–254.
- Edmonds, D. T. and Vollrath, F. (1992). The contribution of atmospheric water vapour to the formation and efficiency of a spider's web. *Proc. R. Soc. Lond.* **248**, 145–148.
- Edwards, G. B. (1984). Large Florida orb-weavers of the genus *Neoscona*. *Entomol. Circ. Fla. Dep. Agric. Consum. Serv.* **266**, 1–2.
- Fischer, F. G. and Brander, J. (1960). Eine Analyse der Gespinste der Kreuzspinne. *Hoppe-Seyler's Z. Physiol. Chem.* **320**, 92–102.
- Fujimori, E. (1965). Ultraviolet light-induced change in collagen macromolecules. *Biopolymers* **3**, 115–119.
- Gleason, D. F., Edmunds, P. J. and Gates, R. D. (2006). Ultraviolet radiation effects on the behavior and recruitment of larvae from the reef coral *Porites astreoides*. *Mar. Biol.* **148**, 503–512.
- Harwood, R. H. (1974). Predatory behavior of *Argiope aurantia* (Lucas). *Am. Midland Nat.* **91**, 130–139.
- Hu, X., Raja, W. K., An, B., Tokareva, O., Cebe, P. and Kaplan, D. L. (2013). Stability of silk and collagen protein materials in space. *Sci. Rep.* **3**, 3428.
- Hudelson, K. (2011). *Ultraviolet Radiation Tolerance in High Elevation Copepods from the Rocky Mountains of Colorado, USA*, Vol. 1520436, p. 70. Ann Arbor: University of North Texas.
- Hylander, S. and Hansson, L.-A. (2013). Vertical distribution and pigmentation of Antarctic zooplankton determined by a blend of UV radiation, predation and food availability. *Aquat. Ecol.* **47**, 467–480.
- Kaur, J., Rajkhowa, R., Tsuzuki, T., Millington, K., Zhang, J. and Wang, X. (2013). Photoprotection by silk cocoons. *Biomacromolecules* **14**, 3660–3667.
- Kuffner, I. B. (2002). Effects of ultraviolet radiation and water motion on the reef coral, *Porites compressa* Dana: a transplantation experiment. *J. Exp. Mar. Biol. Ecol.* **270**, 147–169.
- Liao, C.-P., Blamires, S. J., Hendricks, M. L. and Opell, B. D. (2015). A re-evaluation of the formula to estimate the volume of orb web glue droplets. *J. Arachnol.* **43**, 97–100.
- Ma, Z., Li, W., Shen, A. and Gao, K. (2013). Behavioral responses of zooplankton to solar radiation changes: in situ evidence. *Hydrobiologia* **711**, 155–163.
- Matsuhira, T., Yamamoto, K. and Osaki, S. (2013). Effects of UV irradiation on the molecular weight of spider silk. *Polym. J.* **45**, 1167–1169.
- Opell, B. D. and Hendricks, M. L. (2007). Adhesive recruitment by the viscous capture threads of araneoid orb-weaving spiders. *J. Exp. Biol.* **210**, 553–560.
- Opell, B. D. and Hendricks, M. L. (2009). The adhesive delivery system of viscous capture threads spun by orb-weaving spiders. *J. Exp. Biol.* **212**, 3026–3034.

- Opell, B. D. and Hendricks, M. L. (2010). The role of granules within viscous capture threads of orb-weaving spiders. *J. Exp. Biol.* **213**, 339–346.
- Opell, B. D. and Schwend, H. S. (2007). The effect of insect surface features on the adhesion of viscous capture threads spun by orb-weaving spiders. *J. Exp. Biol.* **210**, 2352–2360.
- Opell, B. D., Karinshak, S. E. and Sigler, M. A. (2011a). Humidity affects the extensibility of an orb-weaving spider's viscous thread droplets. *J. Exp. Biol.* **214**, 2988–2993.
- Opell, B. D., Tran, A. M. and Karinshak, S. E. (2011b). Adhesive compatibility of cribellar and viscous prey capture threads and its implication for the evolution of orb-weaving spiders. *J. Exp. Zool. A Ecol. Genet. Physiol.* **315A**, 376–384.
- Opell, B. D., Karinshak, S. E. and Sigler, M. A. (2013). Environmental response and adaptation of glycoprotein glue within the droplets of viscous prey capture threads from araneoid spider orb-webs. *J. Exp. Biol.* **216**, 3023–3034.
- Opell, B. D., Andrews, S. F., Karinshak, S. E. and Sigler, M. A. (2015). The stability of hygroscopic compounds in orb-web spider viscous thread. *J. Anim. Ecol.* **43**, 152–157.
- Osaki, S. (2004). Ultraviolet rays mechanically strengthen spider's silks. *Polym. J.* **36**, 657–660.
- Osaki, S. and Osaki, M. (2011). Evolution of spiders from nocturnal to diurnal gave spider silks mechanical resistance against UV irradiation. *Polym. J.* **43**, 200–204.
- Otoni, C. G., Avena-Bustillos, R. J., Chiou, B.-S., Bilbao-Sainz, C., Bechtel, P. J. and McHugh, T. H. (2012). Ultraviolet-B radiation induced cross-linking improves physical properties of cold- and warm-water fish gelatin gels and films. *J. Food Sci.* **77**, E215–E223.
- Plateau, J. (1873). *Statique Expérimentale et Théorique des Liquides Soumis aux Seules Forces Moléculaires*, Vol. 1. Paris: Gauthier-Villars.
- Reed, C. F., Witt, P. N. and Scarboro, M. B. (1969). The orb web during the life of *Argiope aurantia*. *Dev. Psychobiol.* **2**, 120–129.
- Sahni, V., Blackledge, T. A. and Dhinojwala, A. (2010). Viscoelastic solids explain spider web stickiness. *Nat. Commun.* **1**, 1–4.
- Sahni, V., Blackledge, T. A. and Dhinojwala, A. (2011). Changes in the adhesive properties of spider aggregate glue during the evolution of cobwebs. *Sci. Rep.* **1**, 41.
- Sahni, V., Dhinojwala, A., Opell, B. and Blackledge, T. (2014). Prey capture adhesives produced by orb-weaving spiders. In *Biotechnology of Silk*, Vol. 5 (ed. T. Asakura and T. Miller), pp. 203–217. Netherlands: Springer.
- Sasaki, M., Kato, N., Watanabe, H. and Yamada, H. (2000). Silk protein, sericin, suppresses colon carcinogenesis induced by 1,2-dimethylhydrazine in mice. *Oncol. Rep.* **7**, 1049–1053.
- Sekiguchi, K. (1952). On a new spinning gland found in geometric spiders and its function. *Annot. Zool. Japonenses* **25**, 394–399.
- Sensenig, A., Agnarsson, I. and Blackledge, T. A. (2010). Behavioural and biomaterial coevolution in spider orb webs. *J. Evol. Biol.* **23**, 1839–1856.
- Shao, Z. and Vollrath, F. (1999). The effect of solvents on the contraction and mechanical properties of spider silk. *Polymer* **40**, 1799–1806.
- Shao, Z., Vollrath, F., Sirichaisit, J. and Young, R. J. (1999). Analysis of spider silk in native and supercontracted states using Raman spectroscopy. *Polymer* **40**, 2493–2500.
- Singaravelan, N., Grishkan, I., Beharav, A., Wakamatsu, K., Ito, S. and Nevo, E. (2008). Adaptive melanin response of the soil fungus *Aspergillus niger* to UV radiation stress at “Evolution Canyon”, Mount Carmel, Israel. *PLoS ONE* **3**, e2993.
- Stellwagen, S. D., Opell, B. D. and Short, K. G. (2014). Temperature mediates the effect of humidity on the viscoelasticity of glycoprotein glue within the droplets of an orb-weaving spider's prey capture threads. *J. Exp. Biol.* **217**, 1563–1569.
- Strutt, J. W. Baron Rayleigh (1892). *Scientific Papers*, Vol. 3, pp. 585–596. Cambridge: Cambridge University Press.
- Swindells, K. and Rhodes, L. E. (2004). Influence of oral antioxidants on ultraviolet radiation-induced skin damage in humans. *Photodermatol. Photoimmunol. Photomed.* **20**, 297–304.
- Tillinghast, E. K. and Christenson, T. (1984). Observations on the chemical composition of the web of *Nephila clavipes* (Araneae, Araneidae). *J. Arachnol.* **12**, 69–74.
- Townley, M. and Tillinghast, E. (2013). Aggregate silk gland secretions of Araneoid spiders. In *Spider Ecophysiology* (ed. W. Nentwig), pp. 283–302. Berlin; Heidelberg: Springer.
- Townley, M. A., Bernstein, D. T., Gallagher, K. S. and Tillinghast, E. K. (1991). Comparative study of orb-web hygroscopicity and adhesive spiral composition in three araneid spiders. *J. Exp. Zool.* **259**, 154–165.
- Tyrrell, R. M. (1995). Ultraviolet radiation and free radical damage to skin. *Biochem. Soc. Symp.* **61**, 47–53.
- Work, R. W. (1981). A comparative study of the supercontraction of major Ampullate silk fibers of orb-web-building spiders (Araneae). *J. Arachnol.* **9**, 299–308.
- Work, R. W. and Morosoff, N. (1982). A physico-chemical study of the supercontraction of spider major ampullate silk fibers. *Textile Res. J.* **52**, 349–356.
- Zhang, Y.-Q. (2002). Applications of natural silk protein sericin in biomaterials. *Biotech. Adv.* **20**, 91–100.
- Zhaorigetu, S., Yanaka, N., Sasaki, M., Watanabe, H. and Kato, N. (2003). Inhibitory effects of silk protein, sericin on UVB-induced acute damage and tumor promotion by reducing oxidative stress in the skin of hairless mouse. *J. Photochem. Photobiol. B* **71**, 11–17.
- Zschokke, S., Hénaut, Y., Benjamin, S. P. and García-Ballinas, J. A. (2006). Prey-capture strategies in sympatric web-building spiders. *Can. J. Zool.* **84**, 964–973.

**Table S1.** Axial deflection angle measurements at 0%, 25%, 50%, 75% and 99% of the droplet extension time for all species and treatment groups (mean $\pm$ 1 s.d.).

	Axial angle 0%	Matched pair 0%	Axial angle 25%	Matched pair 25%	Axial angle 50%
<i>A. aurantia</i>					
Fresh	135.7 $\pm$ 13.1		148.8 $\pm$ 14.8		155.7 $\pm$ 16.5
Dark	133.9 $\pm$ 17.1	$P\geq 0.4927$	142.5 $\pm$ 20.6	<b><math>P\geq 0.0323</math> (4)</b>	150.9 $\pm$ 22.4
Normal UVB	135.9 $\pm$ 20.5	$P\geq 0.5235$	143.2 $\pm$ 23.0	$P\geq 0.0654$	150.4 $\pm$ 26.6
Extreme UVB	140.4 $\pm$ 17.8	$P=0.3035$	147.5 $\pm$ 22.8	$P=0.9906$	152.6 $\pm$ 26.9
<i>L. venusta</i>					
Fresh	116.8 $\pm$ 15.3		116.5 $\pm$ 15.2		114.9 $\pm$ 14.7
Dark	109.6 $\pm$ 14.0	$P\geq 0.0665$	107.7 $\pm$ 13.9	<b><math>P\geq 0.0293</math> (2)</b>	104.9 $\pm$ 14.1
Normal UVB	112.5 $\pm$ 12.6	<b><math>P\geq 0.0380</math> (3)</b>	110.6 $\pm$ 12.1	<b><math>P\geq 0.0209</math> (3)</b>	108.6 $\pm$ 11.9
Extreme UVB	115.5 $\pm$ 10.5	$P=0.8080$	115.0 $\pm$ 10.7	$P=0.7755$	113.8 $\pm$ 10.9
<i>V. arenata</i>					
Fresh	143.1 $\pm$ 9.9		139.1 $\pm$ 11.7		134.1 $\pm$ 13.9
Dark	145.0 $\pm$ 10.3	$P\geq 0.2784$	140.8 $\pm$ 11.6	$P\geq 0.3327$	136.8 $\pm$ 12.9
Normal UVB	141.9 $\pm$ 5.9	$P\geq 0.3492$	137.5 $\pm$ 6.2	$P\geq 0.2841$	133.4 $\pm$ 7.0
Extreme UVB	141.5 $\pm$ 5.6	$P=0.5368$	137.0 $\pm$ 7.2	$P=0.5220$	132.0 $\pm$ 8.5
<i>M. gracilis</i>					
Fresh	114.8 $\pm$ 13.9		117.6 $\pm$ 14.5		115.7 $\pm$ 13.9
Dark	114.3 $\pm$ 13.6	$P\geq 0.3015$	118.7 $\pm$ 14.2	$P\geq 0.1883$	117.1 $\pm$ 16.9
Normal UVB	113.4 $\pm$ 15.5	$P\geq 0.1519$	119.0 $\pm$ 15.3	$P\geq 0.1122$	120.2 $\pm$ 16.5
Extreme UVB	114.6 $\pm$ 11.4	$P=0.9076$	123.4 $\pm$ 16.1	$P=0.1851$	125.0 $\pm$ 16.7
<i>N. crucifera</i>					
Fresh	116.1 $\pm$ 14.1		111.0 $\pm$ 15.6		103.6 $\pm$ 16.5
Dark	124.0 $\pm$ 15.1	$P=0.0951$	122.0 $\pm$ 16.3	<b><math>P=0.0498</math></b>	113.2 $\pm$ 16.3
Extreme UVB	118.0 $\pm$ 19.2	$P=0.6758$	117.5 $\pm$ 21.5	$P=0.2312$	115.2 $\pm$ 21.5

Significant P-values (<0.05) are in bold. Presented for the Normal UVB and Dark treatments are means obtained

by averaging four, 1 h incremental treatment means (due to limited resolution). Individual comparisons were

performed for these hourly treatments, and P-values presented are the lowest of the four comparisons;

parenthesized values indicate which of the four hourly comparisons was significant, if applicable.

**Table S2.** Maximum mean percent axial line elongation as droplets extended during each treatment and the percent extension at which this value was expressed.

	<i>A. aurantia</i>	<i>L. venusta</i>	<i>V. arenata</i>	<i>M. gracilis</i>	<i>N. crucifera</i>
Extension	0%	99%	99%	0%	99%
Fresh	10.6	21.1	12.7	21.2	41.8
Dark					
1 h	10.9	35.8	13.0	17.5	-
2 h	10.6	34.8	9.6	23.3	-
3 h	10.4	33.4	10.8	20.9	-
4 h	12.4	30.7	10.5	26.8	31.0
Normal UVB					
1 h	10.9	28.0	13.1	19.5	-
2 h	9.2	26.2	10.2	24.9	-
3 h	13.4	34.5	12.7	18.4	-
4 h	11.2	24.9	12.6	28.6	-
Extreme UVB	8.5	22.8	12.8	20.1	28.6

For each species, maximum axial line extension occurred at the same percent extension.